Biophysical Chemistry, 32 (1988) 283–295
Elsevier

BPC 01333

Dielectric behavior of polyelectrolytes

VI. Dynamic response of cylindrical biopolymers to electric fields

Wayne E. Sonnen, Gary E. Wesenberg and Worth E. Vaughan

Department of Chemistry, University of Wisconsin – Madison, Madison, WI 53706, U.S.A.

Received 7 June 1988
Accepted 24 October 1988

Polyelectrolyte; Dielectric relaxation; Kerr effect; DNA oligomer; Counterion interaction

The time dependence of the orientation of a cylindrical biopolymer and the configuration of its counterion complement in the presence of an external electric field is found by solving a model forced diffusion equation. The solution is a high temperature expansion in the external field strength and is used to predict the nature of the dielectric relaxation and the dynamic Kerr effect for such systems. Specific application is made to the dynamic Kerr effect of a DNA oligomer for which experimental data appear in the literature. The analysis yields a value for the surface diffusion coefficient of a sodium ion on DNA at 20 °C of 3.8×10^{-10} m^2 s^{-1}.

1. Introduction

The dielectric behavior of natural polyelectrolytes is dominated by the motion of charged species near the surface of the biopolymers. Such motion is an integral component of the biological function of the species. Thus the characterization of the equilibrium and dynamical small ion interactions with the polyelectrolyte and with each other is an obvious first step towards developing a model of the dynamical properties of complex biopolymer assemblies. External electric fields are convenient probes. In the linear regime one can determine the dielectric relaxation and quadratic response to applied fields is exhibited by the Kerr effect. The theory of the equilibrium Kerr effect for spherical and cylindrical model geometries was developed in paper IV [1] and the result applied to experimental data for bovine disk membrane vesicles (DMV) and for DNA oligomers. The dynamical Kerr effect for DMV was considered in paper V [2]. This work presents a general formalism for the dynamical response in cylindrical geometry with a particular application to the dynamic Kerr effect of DNA oligomers.

The model, which has been explored in earlier papers in this series, presumes that a fraction of the counterions are essentially constrained by electrostatic forces to the surface of the polyelectrolyte. These counterions diffuse on the surface and interact with each other via Coulomb forces. In addition the biopolymer executes anisotropic rotational Brownian motion.

From the point of view of statistical mechanics, what is needed to compute macroscopic properties (the Kerr effect response for example) is the joint conditional probability density, i.e. the probability density of finding a configuration of the biopolymer and its counterion complement at time t given a specified configuration at $t = 0$.

2. Evolution of the joint conditional probability density

We seek the time-dependent probability density, P, of finding a molecule (with cylindrical

Correspondence address: W.E. Sonnen, Department of Chemistry, University of Wisconsin–Madison, Madison, WI 53706, U.S.A.

symmetry) with orientation (Euler angles) θ, ϕ and counterion co-ordinates $\{z_i\}$, $\{\phi_i\}$ given the initial state θ', ϕ', $\{z_i'\}$, $\{\phi_i'\}$. With the model picture of rotational diffusion of the molecule and (forced) surface diffusion of the counterions we write

$$\frac{\partial P}{\partial t} = D_\perp \left\{ \frac{1}{\sin\theta} \frac{\partial}{\partial\theta} \sin\theta \frac{\partial P}{\partial\theta} + \frac{1}{\sin^2\theta} \frac{\partial^2 P}{\partial\phi^2} \right\} + (D_\parallel - D_\perp) \frac{\partial^2 P}{\partial\phi^2} + D_1 \sum_i \frac{\partial^2 P}{\partial z_i^2} + \frac{D_1}{b^2} \sum_i \frac{\partial^2 P}{\partial \phi_i^2} + \frac{D_\perp}{k_B T} \frac{1}{\sin\theta} \frac{\partial}{\partial\theta} \times \left[P \sin\theta \frac{\partial V}{\partial\theta} \right] - \frac{E}{k_B T} \frac{\partial}{\partial\phi} \times \Big[P \Big\{ \sin\theta D_\parallel \big[\mu_x \cos\phi - \mu_y \sin\phi \big] - \cot\theta D_\perp \big[\mu_y \cos\theta \sin\phi - \mu_x \cos\theta \cos\phi \big] \Big\} \Big] + \frac{D_1}{k_B T} \left\{ \sum_i P \frac{\partial^2 V}{\partial z_i^2} + \sum_i \frac{\partial P}{\partial z_i} \frac{\partial V}{\partial z_i} + \frac{1}{b^2} \sum_i P \frac{\partial^2 V}{\partial \phi_i^2} + \frac{1}{b^2} \sum_i \frac{\partial P}{\partial \phi_i} \frac{\partial V}{\partial \phi_i} \right\} \tag{1}$$

$D_\perp$ is a component of the (diagonal) rotation diffusion constant tensor that involves motion of the symmetry axis and $D_\parallel$ the component involving motion around the symmetry axis. D_1 is the surface diffusion constant of a counterion. The dipole moment components are (b is the cylinder radius)

$$\mu_x = eb \sum_i \cos\phi_i \quad \mu_y = eb \sum_i \sin\phi_i$$
$$\mu_z = e \sum_i (z_i - L/2) \tag{2}$$

The potential is the interaction with the external field plus the Coulomb repulsions of the counterions

$$V = -E\cos\theta\mu_z - E\sin\theta\sin\phi\mu_x - E\sin\theta\cos\phi\mu_y + V' \tag{3}$$

$$V' = \sum_{ij}{}' \frac{e^2}{4\pi\epsilon\epsilon_0 |r_i - r_j|} \tag{4}$$

The double sum is over pairwise interactions. P can be expanded in a complete set of functions which satisfy the boundary conditions $\partial P/\partial z_i = 0$, $z_i = 0$, L (no flux of probability density at the ends of the cylinder).

$$P = \sum_{Lm\{m_i' n_i'\}} a_{Lm}^{m_1' n_1' m_2' n_2' \cdots} Y_{Lm} \prod_i \cos\frac{m_i' \pi z_i}{L} \exp(i n_i' \phi_i) \tag{5}$$

We seek the time dependence of the expansion coefficients. This can be done conveniently via a high-temperature expansion (power series in E). The dynamics of the individual a values is shown with the aid of the projection operator

$$\int d\Omega Y_{Lm}^* \prod_i \int \frac{(2-\delta_{m0})}{L} \cos\frac{m_i \pi z_i}{L} dz_i \times \int \frac{1}{2\pi} \exp(-i n_i \phi_i)\, d\phi_i \tag{6}$$

The calculation is shown for the cases of (a) removal of a previously applied field and (b) imposition of a step field. Case b includes the reversing field situation. The previous history of the system is contained in the initial conditions.

3. The field off response

The field off response is fairly simple since the forced diffusion equation factors as

$$P = P^1(\theta, \phi) P^2(\{z_i\}, \{\phi_i\}) \tag{7}$$

Clearly P^1 can be expressed as $P^1 = \sum a_{Lm} Y_{Lm}$ and using the projection operator

$$\frac{\partial a_{Lm}}{\partial t} = \big[-L(L+1) D_\perp - m^2 (D_\parallel - D_\perp) \big] a_{Lm} \tag{8}$$

so that

$$a_{Lm}(t) = a_{Lm}(0) \exp\big[-\big(L(L+1) D_\perp + m^2 (D_\parallel - D_\perp) \big) t \big] \tag{9}$$

To calculate the Kerr effect a_{20} suffices since we will argue that the motion of the counterions does

not influence the optical properties of the biopolymer appreciably.

The solution for P^2 is more involved. It will be needed for the prediction of the dielectric relaxation because the motion of the counterions changes the dipole moment of the biopolymer and hence the electrical polarization of the system (of independent molecules).

P^2 satisfies the differential eq. 1 with E, $D_\perp$ and $D_\parallel$ set equal to zero. The expansion of P^2 is

$$P^2 = \sum_{\{m_i', n_i'\}} a^{m_1' n_1' m_2' n_2' \cdots} \prod_i \cos\frac{m_i' \pi z_i}{L} \exp(i n_i' \phi_i) \tag{10}$$

$V/k_B T \equiv V'/k_B T$ is expanded in the same basis

$$V'/k_B T = \sum_{ij}' \sum_{m=0}^{\infty} \sum_{n=-\infty}^{\infty} R_{mn} \exp\big(i n(\phi_i - \phi_j)\big) \times \cos\frac{m\pi z_i}{L} \cos\frac{m\pi z_j}{L} \tag{11}$$

Applying the projection operator (D_1 is absorbed in t)

$$\frac{\partial a^{m_1 n_1 m_2 n_2 \cdots}}{\partial t} = -\left[\sum_i \frac{m_i^2 \pi^2}{L^2} + \frac{\sum_i n_i^2}{b^2}\right] a^{m_1 n_1 m_2 n_2 \cdots} + \sum_{\{m_i', n_i'\}} C^{m_1 n_1 m_2 n_2 \cdots}_{m_1' n_1' m_2' n_2' \cdots} a^{m_1' n_1' m_2' n_2' \cdots} \tag{12}$$

The coupling coefficients C are found by performing the integration indicated by the projection operator including in the integrand the appropriate derivatives of P and V'. Since V' involves only two coordinates at a time the m_i, n_i and m_i', n_i' differ only for the chosen coordinates. Choosing the coordinates to be i and j ($> i$) the second term in eq. 12 becomes

$$\sum_{ij}' \sum_{m=0}^{\infty} \sum_{n=-\infty}^{\infty} \sum_{m_i' n_i' m_j' n_j'} a^{m_1 n_1 \cdots m_i' n_i' m_j' n_j' \cdots} R_{mn} \epsilon C_{m_j' m} \cdot \left\{ \epsilon C_{m_i' m} \left[-\frac{m^2 \pi^2}{L^2} - \frac{n^2}{b^2} - \frac{n n_i'}{b^2} \right] + \epsilon S_{m_i' m} \left[\frac{m m_i' \pi^2}{L^2} \right] \right\} \tag{13}$$

The ϵC and ϵS factors are integrals over cosines and sines reflecting the fact that m_i, m_i', and m (and i) are not independent. Values of ϵC and ϵS are shown in the appendix.

Certain relations between (m_i, m_i', m), (n_i, n_i', n), (m_j, m_j', m) and (n_j, n_j', n) must hold.

$m_i' = m_i + m$ or $m_i' = m_i - m$ or $m_i' = m - m_i$, $m_j' = m_j + m$ or $m_j' = m_j - m$ or $m_j' = m - m_j$; $m_k' = m_k$ etc. $n_i' = n_i - n$; $n_j' = n_j + n$; $n_k' = n_k$ etc. The various m indices are further constrained by the requirement that they be nonnegative. With the range of m and n unconstrained, the evolution of a given expansion coefficient a is coupled to an infinite number of other coefficients. However, the role of the R_{mn} decreases with increasing magnitude of the subscripts and a sufficiently accurate system of working equations can be found by truncating the sum for C at selected values of m and n. The resulting system of coupled linear differential equations for the a values can be solved by standard methods.

To close the calculation we need the initial values of a and values for R_{mn}. The calculation of these quantities is shown in the appendix.

4. The field on response

The expansion coefficients can be expressed as a power series in the field E that is applied at $t = 0$.

$$a_{Lm}^{m_1' n_1' m_2' n_2' \cdots} = {}^0a_{Lm}^{m_1' n_1' m_2' n_2' \cdots} + E^1 a_{Lm}^{m_1' n_1' m_2' n_2' \cdots} + \cdots \tag{14}$$

Coefficients of E in eq. 1 are collected and the resulting equations solved order by order.

4.1. Zero order terms

Eq. 1 is solved for $E = 0$. The solution is

$${}^0P(0) = {}^0P(t) = {}^0P(\infty) = \exp(-V'/k_B T) \Big/ \int \exp(-V'/k_B T)\, d\tau \tag{15}$$

No zero coefficient changes with time. The absence of θ, ϕ dependence in ${}^0P$ means that $L = m = 0$ for all zero order terms. The values of non-vanishing ${}^0a$ are found by applying the projection operator to eq. 15. Values are shown in the appendix.

4.2. First order terms

The projection operator when applied to the various terms of eq. 1 yields

$$\frac{\partial {}^1a_{Lm}^{m_1 n_1 m_2 n_2 \cdots}}{\partial t} = -\left[L(L+1)D_\perp + m^2(D_\parallel - D_\perp) + D_1 \sum_i \frac{m_i^2 \pi^2}{L^2} + D_1 \sum_i \frac{n_i^2}{b^2}\right] {}^1a_{Lm}^{m_1 n_1 m_2 n_2 \cdots} + \sum_i \epsilon_{m_i} \frac{eL}{\sqrt{3}} \frac{2D_\perp}{k_B T} \sum_{m_i'} \left[-\left\{ \frac{1}{(m_i + m_i')^2 \pi^2} + \frac{1}{(m_i - m_i')^2 \pi^2} \right\} {}^0a_{00}^{m_1 n_1 \cdots m_i' n_i' \cdots} \right]$$

for $m_i + m_i'$ odd and $L = 1$, $m = 0$. $\epsilon_m = 2 - \delta_{m0}$.

$$+ \sum_i \frac{ieb}{2} \sqrt{2/3} \left(\frac{D_\parallel + D_\perp}{k_B T} \right) {}^0a_{00}^{m_1 n_1 \cdots m_i n_i - 1 \cdots}$$

for $L = 1$, $m = 1$

$$+ \sum_i \frac{ieb}{2} \sqrt{2/3} \left(\frac{D_\parallel + D_\perp}{k_B T} \right) {}^0a_{00}^{m_1 n_1 \cdots m_i n_i + 1 \cdots}$$

for $L = 1$, $m = -1$

$$+ D_1 \sum_{ij}{}' \sum_{(m_i' n_i')} C_{m_1 n_1 m_2 n_2 \cdots m_i' n_i' m_j' n_j' \cdots}^{m_1 n_1 m_2 n_2 \cdots} {}^1a_{Lm}^{m_1 n_1 \cdots m_i' n_i' m_j' n_j' \cdots}$$

where the C values were found previously (eq. 13).

$$\sum_i \frac{-4\, eL}{k_B T} \frac{D_1}{L^2} \frac{1}{\sqrt{3}} \sum_{k \text{ odd}} {}^0a_{00}^{m_1 n_1 \cdots m_i' n_i \cdots} \frac{m_i'}{k} \epsilon S_{m_i m_i' k}$$

for $m_i' = m_i + k$ or $m_i' = m_i - k$ or $m_i' = k - m_i$ and $L = 1$, $m = 0$.

$$+ \sum_i \frac{ieb}{2} \frac{D_1}{b^2} \frac{n_i}{k_B T} \sqrt{2/3}\, {}^0a_{00}^{m_1 n \cdots m_i n_i - 1 \cdots}$$

for $L = 1$, $m = 1$.

$$+ \sum_i \frac{ieb}{2} \frac{D_1}{b^2} \frac{n_i}{k_B T} \sqrt{2/3}\, {}^0a_{00}^{m_1 n_1 \cdots m_i n_i + 1 \cdots}$$

for $L = 1$, $m = -1$.

$$\sum_i \frac{4\, eL}{k_B T} \frac{D_1}{L^2} \frac{1}{\sqrt{3}} \sum_{k \text{ odd}} {}^0a_{00}^{m_1 n_1 \cdots m_i' n_i \cdots} \frac{m_i'}{k} \epsilon S_{m_i m_i' k} \quad (16)$$

for $k = m_i + m_i'$ or $k = m_i' - m_i$ or $k = m_i - m_i'$ and $L = 1$, $m = 0$.

This system is of the same form as eq. 12 and is easily solved with the initial conditions ${}^1a(0) = 0$.

4.3. Second order terms

We exhibit the equation of change of the expansion coefficient for $L = 2$, $m = 0$ and $\{m_i, n_i\} = 0$ since this single coefficient suffices to compute the (low field) Kerr effect of the system. The result is (the first contribution to a_{20} is second order in E)

$$\frac{\partial {}^2a_{20}^{0000 \cdots}}{\partial t} = -6D_\perp {}^2a_{20}^{0000 \cdots} - \sum_i \frac{4eL}{\pi^2} \frac{D_\perp}{k_B T} \sqrt{3/5} \times \sum_{m_i' \text{ odd}} \frac{{}^1a_{10}^{00 \cdots m_i' 0 \cdots}}{m_i'^2}$$

$$\sum_i ieb \frac{D_\perp}{k_B T} \sqrt{3/10} \left\{ {}^1a_{11}^{00 \cdots 01 \cdots} + {}^1a_{1-1}^{00 \cdots 0-1 \cdots} \right\} \quad (17)$$

The solution for the required ${}^1a(t)$ and then for ${}^2a_{20}^{0000 \cdots}(t)$ is straightforward. Results are shown in the appendix.

5. The Kerr effect – field off response

Our picture is that the optical anisotropy of DNA oligomers arises from the fixed structure of the DNA double helix and is independent of the configuration of the counterions. The counterion

distribution (in the presence of the external field) does influence the interaction with the field and thereby the initial (equilibrium) value of the optical phase shift. This is directly related to the orientation function $\langle P_2(\cos\theta)\rangle = \Phi$ via

$$\frac{\delta_S}{\delta_E} = \Phi \tag{18}$$

where δ_E is the optical phase shift in the presence of the external field and δ_S its saturation value for a given system. When the field is removed, the motion of the counterions does not affect the decay of Φ which is completely controlled by the rotational diffusion of the symmetry axis of the cylinder (rod). Thus Φ decays exponentially with a rate $6D_\perp$. An illustration of this behavior for a 42.2 nm DNA fragment at 20 °C in 1 mM NaP at pH 7.0 appears in the literature [3]. The field off response fits a single exponential well. The reported value [3] is $D_\perp = 1.28 \times 10^5\ s^{-1}$. Regression on the field off data taken (by digitization) from fig. 3 of ref. 3 gave $D_\perp = 1.47 \times 10^5\ s^{-1}$ which agrees with the previous value within the accuracy of the procedure.

Since the DNA oligomers are large compared to the solvent molecules, one can use a hydrodynamical expression to predict the length dependence of $D_\perp$ and thereby test our molecular picture of the dynamics. An appropriate expression is the Kirkwood–Auer–Riseman equation [4]

$$D_\perp = \frac{3k_BT\ \ln(N_wL_0/2b)}{\pi\eta_0 N_w^3 L_0^3} \tag{19}$$

where b approximates the molecular radius, N_w is the weight average degree of polymerization, η_0 is the solvent viscosity, and L_0 the monomeric projection length. Since data for only one length are reported in ref. 3 the L dependence of $D_\perp$ cannot be examined. However, eq. 19 can be used directly, and we calculate $D_\perp = 1.42 \times 10^5\ s^{-1}$ in good agreement with the experimental value.

An alternative expression for $D_\perp$, with correction for end effects, has been reported by Tirado et al. [5] (a (negative) term $\delta_\perp$ is added to $\ln(N_wL_0/2b)$). Use of that formula yields $D_\perp = 1.02 \times 10^5\ s^{-1}$ in poorer agreement with the experimental value, but still reasonable considering the dependence on N_w^3 in eq. 19.

Table 1
Initial values of the orientation function as a function of field

E (V/m)	$\Phi(\infty)$	E (V/m)	$\Phi(\infty)$
1×10^4	0.000	2×10^6	0.779
5×10^5	0.067	4×10^6	0.949
8×10^5	0.175	1×10^7	0.993
1×10^6	0.278	1×10^8	0.998
1.5×10^6	0.581		

The value of $\Phi(\infty)$ is easily calculated (by Monte-Carlo integration) as

$$\Phi = \int P_2(\cos\theta)\ \exp(-V/k_BT)\ d\tau / \int \exp(-V/k_BT)\ d\tau \tag{20}$$

where V is given by eq. 3. Values of $\Phi(\infty, E)$ for $t = 20$ °C and $L = 42.2$ nm are shown in table 1.

Exponential decay in the field off regime is *not* found for all systems. With large external fields, the field off decay of the optical phase shift of bovine disk membrane vesicles is decidedly nonexponential as a result of a significant contribution to the optical anisotropy of a vesicle from the distortion of the distribution of the charged rhodopsin molecules embedded in the membrane [2].

The initial value of the orientation function for cylindrical biopolymers with associated counterions depends on the length L, number of counterions n', and the temperature in addition to the electric field E. We have calculated $\Phi(\infty)$ for various combinations of these variables.

The temperature is a relatively unimportant variable. Higher temperatures reduce slightly the role of the dipole–field and counterion–counterion interactions as can be seen from eq. 20. For DNA, the condensation model assumption means that n' and L are not both independent variables, but $n' = 0.76L/0.17$ (L in nm). With some other polyelectrolytes, separate control of n' and L is possible.

The orientation function remains small until the interaction energies with the field become

comparable to the counterion repulsion energies. At this point the orientation function increases rapidly as the field is increased. This pattern is similar to that found for bovine disk membrane vesicles [2] and the rapid change of a macroscopic system function (orientation function) with a system variable (external electric field) is characteristic of co-operative phenomena. The data of table 1 illustrate the rapid onset of saturation of the orientation function. Similar behavior is found for smaller L.

The other significant trend is the field strength required to establish a given value for the orientation function as a function of L. Not surprisingly, since smaller L (for DNA) requires smaller n', the field increases as L decreases. Saturation of the orientation function takes place long before one sees gross displacement of the counterion distribution towards one end of the cylinder. Thus the induced dipole moment, in the regime where the orientation function is changing rapidly, is roughly proportional to L. These observations argue that EL should be a constant for fixed Φ, i.e. the plot of Φ versus log E should be displaced by $\log(L_1/L_2)$. This picture fits the calculated curves well. For very short oligomers, the ϕ direction becomes the 'long' direction and the saturating value of the orientation function becomes -0.5. As this regime is approached, 'end effects' will cause the simple picture presented above to break down.

6. Dielectric behavior

The dielectric behavior is given by the (unnormalized) dipolar correlation function

$$\gamma = \sum_{\{m_i,\, n_i\}} \{ a_{10}^{m_1 n_1 \cdot}(0)\, a_{10}^{m_1 n_1 \cdot}(t) + a_{11}^{m_1 n_1 \cdot}(0)\, a_{11}^{m_1 n_1 \cdot}(t) + a_{1-1}^{m_1 n_1 \cdot}(0)\, a_{1-1}^{m_1 n_1 \cdot}(t) \} \tag{21}$$

evaluated using the field off decay. Recall that the expansion coefficients factor $a_{Lm}^{m_1 n_1 \cdots} = a_{Lm} a^{m_1 n_1}$ reflecting the fact that independent processes are taken place, both reducing the electric polarization (system dipole moment). One is the reorientation of dipoles which is expressed in the formalism by

$$\frac{a_{10}(t)}{a_{10}(0)} = \exp(-2D_\perp t)\frac{a_{11}(t)}{a_{11}(0)} = \frac{a_{1-1}(t)}{a_{1-1}(0)}\exp\left(-\left[D_\parallel + D_\perp\right]t\right) \tag{22}$$

These are the usual Perrin model results for the anisotropic rotational diffusion of a spheroidal molecule with dipole moment components along all symmetry axes.

The other process is the decay of the dipole moment components given by the $a^{m_1 n_1 \cdot}(t)$. Only those a values for which $a^{m_1 n_1 \cdot}(0)$ is nonvanishing are needed. In terms of the high temperature expansion we want contributions from the following integral

$$\frac{E}{1!k_B T}\int Y_{Lm}\prod_i \cos\frac{m_i \pi z_i}{L}\exp(-in_i\phi_i) \cdot \left\{\cos\theta\, eL\sum_i (z_i - L/2) + \sin\theta\,\sin\phi\, eb\sum_i \cos\phi_i + \sin\theta\,\cos\phi\sum_i \sin\phi_i\right\} \mathrm{d}\tau \tag{23}$$

Obviously only $L = 1$ ($m = 0, \pm 1$) are allowed. In addition, only one n_i can be nonzero and its value is ± 1. Similarly only one m_i can be nonzero and its value must be odd. Thus the scope of the calculation is greatly reduced. Since we do not yet have experimental dielectric data for comparison to the theory, evaluation of the time dependence of the a values is not pursued. The evaluation of these terms is similar to the (field on) calculation shown in the appendix (section A5).

7. The Kerr effect – field on response

The structure of the forced diffusion equation causes ${}^2a_{00}^{0000\cdots}(t)/{}^2a_{00}^{0000\cdots}(\infty) = P_2(t)/P_2(\infty)$ to be a sum of exponentials with time constants and amplitudes closely related to those causing the dielectric behavior (see eqs. A9 and A10). What one finds is change in ${}^2a_{00}^{0000\cdots}(t)$ caused by rotational diffusion involving motion of the z-axis

(rate $6D_\perp$) and coupled motions involving the ϕ coordinates of the cylinder and the counterions (rates a function of $D_\perp$, $D_\parallel$ and D_1) and involving the θ coordinate of the cylinder and the z coordinates of the counterions (rates a function of $D_\perp$ and D_1). A single term (see eq. A12) describes the contribution from motions involving changes in ϕ and $\{\phi_i\}$. Its amplitude is about 1–2 orders of magnitude smaller than that of other terms and its rate about 2 orders of magnitude larger. Thus it represents a small short time effect on the (field on) dynamic Kerr effect. This is the *only* term involving $D_\parallel$ so an estimate of the value of $D_\parallel$ is not critical to the analysis. A series of exponentials with relatively slow rates (see section A5) describes the effect of the counterion motions changing $\{z_i\}$. Thus our formalism predicts the (small) field on dynamic Kerr effect to show single exponential small amplitude short time response followed by growth described by a sum of exponentials (see section A5 for typical values). Note that it is not necessary to know the actual value of the electric field strength (the relation between the applied field strength and the local (Maxwell) field strength is an unsolved problem for the Kerr effect) since it cancels in the quotient of ^2a. The quotient, however, is a function of the dynamical variables of interest ($D_\perp$, $D_\parallel$ and D_1).

To implement the formalism we require values for $D_\perp$, $D_\parallel$ and $D_1 \cdot D_\perp$ is known from the field off behavior so we are left with two adjustable parameters. $L = 42.16$ nm, $b = 1.3$ nm and $n' = 188$ are fixed in advance. Clearly $D_\parallel$ will be considerably larger than $D_\perp$ – we estimate $D_\parallel = 10^7$ s^{-1}. An accurate estimate of $D_\parallel$ is not required since it affects the model equation very weakly. In turn if $D_\parallel$ is treated as a parameter in regression, its value is very uncertain. D_1 is expected to be much smaller than the 1.3×10^{-9} m^2 s^{-1} value for the diffusion of sodium ions in water at 20 °C – we guessed [6] $D_1 = 10^{-11}$ m^2 s^{-1} previously. Here D_1 is used as a fitting parameter in a regression analysis.

The model of ref. 3 reduces the dimensionality of the counterion coordinates to one (!) with the result that the long time behavior is predicted to be a single exponential. In table 2 we show $P_2(t)/P_2(\infty)$ as a function of t for data taken from fig. 3 of ref. 3, the same quantity calculated from the model of ref. 3 using values for the model parameters reported therein, and as determined via regression (setting $D_\perp = 1.28 \times 10^5$ s^{-1}) using our formalism. We find $D_1 = 4.8 \times 10^{-10}$ m^2 s^{-1} and a sum of squared residuals of 3.162×10^{-2}. If $D_\perp$ as well as D_1 are allowed to vary in the regression, we find $D_\perp = 1.38 \times 10^5$ s^{-1} and $D_1 = 3.78 \times 10^{-10}$ m^2 s^{-1} and a sum of squares of 3.011×10^{-2}. A fit of the model of ref. 3 gives a sum of squares of 9.337×10^{-2}. A better fit could be found if the parameter τ describing the 'ion atmosphere' relaxation were determined by fitting only the field on data instead of the combined field on and field reversal data. The residuals as a function of time for each model are

Table 2

Dynamic Kerr effect – field on response ($D_\perp = 1.28(10)^5$ s^{-1})

t (μs)	$P_2(t)/P_2(\infty)$		
	Experiment	Model of ref. 3	Present work
0.2463	0.0063	0.1041	0.0815
0.2934	0.0335	0.1326	0.1025
0.3842	0.0673	0.1876	0.1450
0.3903	0.1046	0.1912	0.1479
0.4800	0.1317	0.2436	0.1912
0.4844	0.1588	0.2461	0.1934
0.5775	0.2062	0.2974	0.2385
0.6273	0.2503	0.3236	0.2625
0.6777	0.2977	0.3492	0.2864
0.7696	0.3383	0.3934	0.3292
0.8616	0.3790	0.4347	0.3704
0.9563	0.4366	0.4744	0.4111
1.0920	0.4839	0.5264	0.4658
1.2299	0.5448	0.5740	0.5171
1.4094	0.5989	0.6288	0.5773
1.5002	0.6328	0.6538	0.6051
1.6342	0.6700	0.6877	0.6430
1.7688	0.7105	0.7183	0.6776
1.9455	0.7477	0.7541	0.7181
2.2075	0.7847	0.7989	0.7692
2.4695	0.8218	0.8355	0.8111
2.7725	0.8486	0.8697	0.8502
3.0323	0.8721	0.8932	0.8773
3.4206	0.8988	0.9208	0.9089
3.8078	0.9188	0.9411	0.9323
4.1518	0.9354	0.9548	0.9486
4.5374	0.9452	0.9664	0.9614
4.9661	0.9583	0.9758	0.9722
5.4375	0.9714	0.9831	0.9806
6.1649	0.9842	0.9903	0.9889

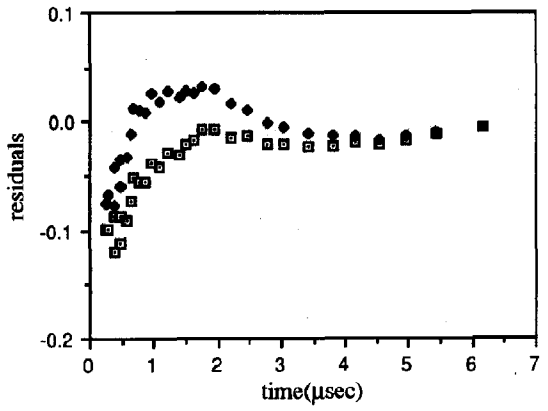

Fig. 1. Dynamic Kerr effect – field on response. Residuals (experimental values minus model calculation) as a function of time. (◆) Present work; (□) data of ref. 3.

shown in fig. 1. Examination of the residuals shows that they are consistently smaller for the present work. However, even though the quality of fit is good, both calculations show obvious systematic trends in the residuals. The origin of these systematic deviations is uncertain although the model does not treat some system properties (see below) which could influence the dynamic Kerr effect to an extent exceeding the error of measurement. By virtue of having the field reversal data as input to the regression parameters of ref. 3, the residuals obtained from the model of ref. 3 do not even add to zero but are all negative.

8. Conclusions

A molecular dynamical model employing the full configuration space of the coordinates of a cylindrical polyelectrolyte and its complement of counterions was evaluated by a high temperature expansion through second order in the applied field. Low field data for the dynamical Kerr effect of a particular DNA oligomer are taken from the literature and regression on the field on data yields $D_\perp = 1.38 \times 10^5$ s^{-1} for the significant component of the rotational diffusional tensor of the cylinder and $D_1 = 3.8 \times 10^{-10}$ for the surface diffusion coefficient of a sodium ion (20 °C). Regression on the field off data gave $D_\perp = 1.47 \times 10^5$ s^{-1}, calculation via the Kirkwood–Auer–Riseman equation gave $D_\perp = 1.42 \times 10^5$ s^{-1} and calculation from the equation of Tirado et al. gave $D_\perp = 1.02 \times 10^5$ s^{-1}. The current model contains two adjustable dynamical parameters which affect the fit as does the model of ref. 3 in which the counterion coordinates are lumped into a effective single coordinate whose change in time is described by an empirical parameter. The current model is molecular rather than empirical in its description of the dynamics and accounts for motion in the ϕ_i coordinates as well as z_i.

The value found for D_1 is considerably larger than a guess [6] $D_1 = 10^{-11}$ m^2 s^{-1} and a similar value extracted by an approximate argument from the relaxation time of the effective coordinate reported in ref. 3 [7] ($D_1 = 1.1 \times 10^{-11}$ m^2 s^{-1}). In retrospect this second estimate of D_1 was unreasonably low. The collective diffusion of a large number of counterions causes a fluctuation in dipole moment along the long axis to decay to zero. The decay of the dipole moment will occur more slowly than the loss of correlation of the position of a single counterion with its position at an earlier time. Roughly, for a random walk, if the standard deviation for diffusion of a single particle is σ, then that of the mean position of a collection (n') of particles (same distance scale) is $\sigma/\sqrt{n'}$ [8]. But the relation $\sigma^2 = 2Dt$ means $2D_1 t = 2Dn't$ so the 'diffusion constant' for the system (z-direction) dipole moment will be n' smaller than D_1. Thus the number to be compared to 1.1×10^{-11} m^2 s^{-1} is $D_1/n' = 2.0 \times 10^{-12}$. The comparison is about as good as could be expected considering the approximate nature of the several models glued together.

For $L = 42.16$ nm the present calculation effectively contains two exponentials (rate $6D_\perp$ and λ_1). This is caused by the large value of L ($-\lambda_1$ is the relaxation rate of the dominant term arising roughly from motion of the counterions along the long axis of the cylinder). With smaller L, $D_\perp$ increases more rapidly than the contribution of D_1 to the λ_i (the longitudinal rates), the relaxation rates come close together and the amplitudes of terms other than $m_1(A_1, \lambda_1)$ become relatively larger. Furthermore shorter oligomers are more rigid and the assumption of cylindrical geomtery will be more reasonable.

We have ignored the presence of the phosphate groups in this formalism. However, a calculation of the equilibrium low field Kerr effect [1] from the same molecular picture in which the phosphate distribution was successively (1) ignored, (2) modeled by a continuous line charge down the cylinder axis, and (3) modeled by point charges on an idealized double helix 1.0 nm away from the axis showed only small differences in calculated quantities. The phosphate charges only serve to constrain the counterions to the surface of the cylinder. We found previously [9] that the condensation model number of counterions, constrained to the surface of a cylinder of dimensions corresponding to that of DNA, in the absence of auxiliary charges, had a minimum energy configuration of a double helix in registry with that of the (absent) phosphate distribution. Thus the phosphates are not needed to make the double helical counterion configuration energetically favorable.

The interaction of the remaining 24% of the counterions has been ignored in this work although it was treated in part in an earlier calculation aimed at deriving an expression for the dipolar correlation function [6] to predict the dielectric relaxation. That work involved analysis of fluctuations at equilibrium and did not include interaction with electric fields. With external fields, the diffusion of free ions in bulk is perturbed, establishing flows which, in the steady state, contribute to the system polarizability and hence to the birefringence [10–12]. Furthermore the field dependence of the orientation function is distinctly different for the free ion atmosphere mechanism [12]. Our calculation treats the condensed counterion polarization alone and is (as are previous calculations of this type) an equilibrium rather than a steady state analysis. For low ionic strengths Ray and Charney [11] state that the condensed counterion polarization and the ion atmosphere polarizations are additive. Data are shown in ref. 11 which allow an estimate of the relative importance of the two mechanisms in controlling the birefringence (or electric dichroism). The experimental data analyzed in this work are for a pH 7.0 phosphate buffer solution with $[Na^+] = 1.00 \times 10^{-3}$ M at 20 °C for which we compute the Debye shielding length $1/\kappa$ to be about 8.5 nm. Examination of fig. 12 of ref. 11 (showing the relative importance of the two mechanisms) and allowing for the difference in length (81.6 nm in ref. 11 and 42.16 nm here) suggests that the counterion condensation polarization is the dominant mechanism for the experimental data analyzed in this work.

A referee questioned the appropriateness of the (reflecting) boundary condition $\partial P/\partial x = 0$ at the cylinder ends if the possibility of steady flow on and off the cylinder in the z-direction existed (while maintaining the number of condensed counterions fixed). We agree that this boundary condition would be incorrect if appreciable coupling between longitudinal counterion motion and longitudinal free ion flow existed. The value of $1/\kappa$ computed above suggests that free ion flow is sufficiently small so that it can be neglected. The boundary condition $\partial P/\partial z = K$ would admit sine terms into the basis set, their role increasing with larger values of the flow (described by the constant K).

Appendix A: Mathematical details

A1. Evaluation of the expansion coefficients of the Coulomb potential

Two expressions for the potential energy of interaction of the counterions are [13]

$$\frac{V'}{k_B T} = \sum_{ij}{}' \sum_{m=0}^{\infty} \sum_{n=-\infty}^{\infty} R_{mn} \exp\big(in(\phi_i - \phi_j)\big) \times \cos\frac{m\pi z_i}{L} \cos\frac{m\pi z_j}{L}$$

$$= \sum_{ij}{}' \frac{e^2}{2\pi^2 \epsilon\epsilon_0 k_B T} \sum_{n=-\infty}^{\infty} \int_0^{\infty} dk \times \cos\big(k(z_i - z_j)\big) \exp\big(in(\phi_i - \phi_j)\big) \times I_n(kb) K_n(kb) \qquad \text{(A1)}$$

Since R_{mn} does not depend on i or j or the

number of counterions n', we can apply the projection operator to the ijth term with the result

$$R_{mn} = \frac{e^2\epsilon_m^2}{L^2\pi^2\epsilon\epsilon_0 k_B T}\int_0^\infty dk I_n(kb) \times K_n(kb)\frac{k^2}{\left[k^2-(m\pi/L)^2\right]^2} \times\left[1-(-1)^m\cos(kL)\right] \quad (A2)$$

Eq. A2 is a straightforward one-dimensional (numerical) integral. I_n and K_n are modified Bessel functions of the first and second order respectively and are available as series [14]. The R_{mn} were also found (but with lower accuracy) by Monte Carlo integration on the left hand side of eq. A1 with a projection operator

$$\int d\phi_i \int d\phi_j \cos\left(n(\phi_i-\phi_j)\right)\int dz_1 \cos\frac{m\pi z_1}{L} \times\int dz_2 \cos\frac{m\pi z_2}{L} \quad (A3)$$

Note that $R_{mn} = R_{m-n}$. Some values of R_{mn} for the experimental case to which the formalism is applied are shown in table A1. Values from $m = 0$–50 and $n = 0$–8 were calculated for this and other DNA lengths and temperatures and are stored in computer files.

A2. ϵC and ϵS

When the projection operator (eq. 6) is applied to the last term of eq. 1, the following integrals result:

$$\int_0^L \frac{(2-\delta_{m_i0})}{L}\sin\frac{m_i'\pi z_i}{L}\sin\frac{m\pi z_i}{L}\cos\frac{m_i\pi z_i}{L}dz_i = \epsilon S_{m,m_i'm} \quad (A4)$$

$$\int_0^L \frac{(2-\delta_{m_i0})}{L}\cos\frac{m_i'\pi z_i}{L}\cos\frac{m\pi z_i}{L}\cos\frac{m_i\pi z_i}{L}dz_i = \epsilon_{m,m_i'm} \quad (A5)$$

Nonvanishing values of ϵC and ϵS are shown in table A2.

Table A1

Values of R_{mn} for $L = 42.2$ nm, $b = 1.3$ nm, $t = 20\,^\circ$C

m	n				
	0	1	2	3	4
0	0.43147	0.06557	0.03329	0.02228	0.01674
1	0.13607	0.03170	0.01645	0.01106	0.00833
2	0.10895	0.03103	0.01638	0.01104	0.00832
3	0.08925	0.03013	0.01627	0.01101	0.00831
4	0.07523	0.02912	0.01612	0.01097	0.00829
5	0.06462	0.02804	0.01594	0.01091	0.00827

Table A2

Values of trigonometric integrals

$\epsilon C_{000} = 1$	$\epsilon S_{000} = 0$
$\epsilon C_{0mm} = 1/2$	$\epsilon S_{0mm} = 1/2$
$\epsilon C_{mk,mk,0} = 1$	$\epsilon S_{mk,mk,0} = 0$
$\epsilon C_{mk,0,mk} = 1$	$\epsilon S_{mk,0,mk} = 0$
$\epsilon C_{m,2m,m} = 1/2$	$\epsilon S_{m,2m,m} = 1/2$
$\epsilon C_{mk,m-mk,m} = 1/2\, m > m_k$	$\epsilon S_{mk,m-mk,m} = 1/2\, m > m_k$
$\epsilon C_{mk,mk-m,m} = 1/2\, m_k > m$	$\epsilon S_{mk,mk-m,m} = -1/2\, m_k > m$
$\epsilon C_{mk,mk+m,m} = 1/2$	$\epsilon S_{mk,mk+m,m} = 1/2$
other cases = 0	other cases = 0

A3. Initial values

For the *field on* calculation

$$P(0) = \exp(-V'/k_BT)/\int\exp(-V'/k_BT) = \sum a_{00}^{m_1'n_1'\cdots}(0)\,Y_{00}\prod_i\cos\frac{m_i'\pi z_i}{L}\exp(in_i'\phi_i) \quad (A6)$$

and the $a^{m_1'n_1'm_2'n_2'}(0)$ were found by Monte Carlo integration using the projection operator eq. A3 ($L = m = 0$) for desired selections of $\{m_i', n_i'\}$.

To analyze the dynamic Kerr effect by finding ${}^2a_{20}^{0000\cdots}(t)$, only a subset of the $a^{m_1'n_1'\cdots}(0)$ need be evaluated. We need $a^{m_10m_20\cdots}$ for m_1 even and $m_2 = 0$, and for m_1 and m_2 both odd. $a^{010-1\cdots} + a^{0-101\cdots}$ is also needed. The leading terms of these types (for $L = 42.2$ nm, $b = 1.3$ nm and $t = 20\,^\circ$C) are shown in table A3 (values multiplied by $-(4\pi)^{0.5}\times 10^3$). Additional values are stored in

Table A3

Initial values for the field on dynamics $a_{00}^{010-1\cdots} + a_{00}^{0-101\cdots} = 7.892\ a_{00}^{m_1 0 m_2 0\cdots}$

m_2	m_1				
	2	4	6	8	10
0	−138	−104	−92	−82	−84
m_2	m_1				
	1	3	5	7	9
1	2.77	0.70	0.60	0.51	0.51
3	–	2.55	0.64	0.51	0.47
5	–	–	2.58	0.60	0.62
7	–	–	–	2.43	0.65
9	–	–	–	–	2.24

computer files. The last part of the table is symmetric in the indices m_1 and m_2.

For the *field off* calculation

$$P(0) = \exp(-V/k_B T)/\int \exp(-V/k_B T)\,\mathrm{d}\tau = \sum a_{Lm}^{m_1' n_1' m_2' n_2'}(0)\, Y_{Lm}^{*} \prod_i \cos\frac{m_i' \pi z_i}{L} \exp(i n_i' \phi_i) \tag{A7}$$

and the initial values of a as a function of n', E and L were found by Monte Carlo integration. Some sample values are shown in table A4.

Table A4

Initial values. $n' = 10$, $t = 25\,^\circ$C. Entries are divided by $(4\pi)^{0.5}$. Length L in nm

E (V/m)	$a_{00}^{1010\cdots}(0)$			$1/2[a_{00}^{010-1\cdots} + a_{00}^{0-101\cdots}]$		
	5.1 nm	10.2 nm	20.4 nm	5.1 nm	10.2 nm	20.4 nm
7×10^7	0.786	–	–	0.12	–	–
5×10^7	0.659	0.844	–	0.05	–	–
3×10^7	0.293	0.718	–	−0.029	0.15	–
2×10^7	0.107	0.493	0.736	−0.034	0.009	–
1×10^7	−0.005	0.121	0.519	−0.040	−0.034	0.06
7×10^6	−0.020	0.036	0.312	−0.044	−0.030	−0.006
5×10^6	−0.027	−0.011	0.154	−0.046	−0.030	−0.019
3×10^6	−0.032	−0.022	0.028	−0.048	−0.031	−0.019
2×10^6	−0.033	−0.028	−0.005	−0.048	−0.032	−0.019
1×10^6	−0.034	−0.031	−0.022	−0.049	−0.032	−0.019
7×10^5	−0.034	−0.032	−0.025	−0.049	−0.032	−0.019
5×10^5	−0.034	−0.032	−0.026	−0.049	−0.032	−0.019
3×10^5	−0.034	−0.032	−0.027	−0.049	−0.032	−0.019

A4. Evaluation of ${}^2a_{20}^{0000\cdots}(t)$

Since all counterions are equivalent eq. 17 becomes

$$\frac{\partial^2 a_{20}^{0000\cdots}}{\partial t} + 6D_\perp {}^2a_{20}^{0000\cdots} = -\frac{4eLn'}{\pi^2}\frac{D_\perp}{k_B T}\sqrt{3/5}\sum_{k\ \mathrm{odd}}\frac{{}^1a_{10}^{k000\cdots}}{k^2} + in'eb\frac{D_\perp}{k_B T}\left\{{}^1a_{11}^{0100\cdots} + {}^1a_{1-1}^{0-100\cdots}\right\} \tag{A8}$$

This is of the form

$$\frac{\mathrm{d}y}{\mathrm{d}t} + Py = \sum_i A_i(1 - \exp(\lambda_i t)) \tag{A9}$$

with the solution

$$y = \exp(-6D_\perp t)\sum_i A_i\left\{\frac{\exp(6D_\perp t) - 1}{6D_\perp} - \frac{\exp((6D_\perp + \lambda_i)t) - 1}{6D_\perp + \lambda_i}\right\} \tag{A10}$$

The A_i and λ_i are found by analysis of the first order terms.

A5. The first order terms

Ignoring (for the moment) the terms involving R_{mn}, eq. 16 applied to the required first order terms yields

$$\frac{\partial {}^1a_{11}^{0100\cdots}}{\partial t} = -\left[D_\parallel + D_\perp + \frac{D_1}{b^2}\right]{}^1a_{11}^{0100\cdots} + \left[\frac{ieb}{2}\sqrt{2/3}\,\frac{1}{\sqrt{4\pi}}\,\frac{D_\parallel + D_\perp + D_1/b^2}{k_B T} + \frac{ieb}{2}\sqrt{2/3}\,(n'-1)\frac{D_\parallel + D_\perp}{k_B T}\right]{}^0a_{00}^{010-1\cdots} \tag{A11}$$

with a similar expression for ${}^1a_{1-1}^{0-100\cdots}$. Thus

$$
\begin{aligned}
&{}^1a_{11}^{0100\cdots} + {}^1a_{1-1}^{0-100\cdots} \\
&= \left\{ \frac{ieb}{k_B T}\sqrt{2/3}\,\frac{1}{\sqrt{4\pi}} + \frac{ieb}{2}\sqrt{2/3}\,\frac{(n'-1)}{k_B T} \right. \\
&\quad \times \frac{D_{\parallel} + D_{\perp}}{D_{\parallel} + D_{\perp} + D_1/b^2} \\
&\quad \left. \times \left[{}^0a_{00}^{010-1\cdots} + {}^0a_{00}^{0-101\cdots} \right] \right\} \\
&\quad \cdot \left[1 - \exp\left\{ -\left[D_{\parallel} + D_{\perp} + D_1/b^2 \right] t \right\} \right] \qquad \text{(A12)}
\end{aligned}
$$

The remaining terms are (m_1 odd)

$$
\begin{aligned}
&\frac{\partial\, {}^1a_{10}^{m_1000\cdots}}{\partial t} \\
&= -\left[2D_{\perp} + \frac{D_1 m_1^2 \pi^2}{L^2} \right] {}^1a_{10}^{m_1000\cdots} \\
&\quad + \sum_{m_1' \text{ even}} \frac{2eL}{\sqrt{3}}\,\frac{2D_{\perp}}{k_B T} \left[-\left\{ \frac{1}{(m_1 + m_1')^2 \pi^2} \right. \right. \\
&\quad \left. \left. + \frac{1}{(m_1 - m_1')^2 \pi^2} \right\} \right] {}^0a_{00}^{m_1'000\cdots} \\
&\quad + \sum_{m_2' \text{ odd}} \frac{2eL}{\sqrt{3}}\,\frac{2D_{\perp}}{k_B T}(n'-1) \left[-\frac{2}{m_2'^2 \pi^2} \right] \\
&\quad \times {}^0a_{00}^{m_1 0 m_2' 0\cdots} \\
&\quad + \sum_{k \text{ odd},\, m_1' \text{ even}} \frac{4eL}{\sqrt{3}}\,\frac{D_1}{L^2 k_B T} \left[-\epsilon C_{m_1 m_1' k} \right. \\
&\quad \left. + \frac{m_1'}{k} \epsilon S_{m_1 m_1' k} \right] {}^0a_{00}^{m_1'000\cdots} \qquad \text{(A13)}
\end{aligned}
$$

Using the final regression value of $D_1 = 4.90 \times 10^{-10}$ m^2 s^{-1} fixing $D_{\perp} = 1.28 \times 10^5$ s^{-1} and $D_{\parallel} = \times 10^7$ s^{-1}, eqs. A12 and A13 yield (see eq. A10) values of A_i and λ_i.

From the entries of table A5 it would appear that a number of terms influence the calculation of Φ. However, inspection of eq. A10 shows that $y(t)/y(\infty)$ has $A_i/\sum A_i$ divided by $1 + \lambda_i/6D_{\perp}$ in the terms with rate constants $-\lambda_i$. Since $-\lambda_i$ is large compared to $6D_{\perp}$ for all terms except that for $i = 1$, the final solution contains effectively two significant exponentials (rate constants $6D_{\perp}$ and λ_1) and a collection of small amplitude rapidly decaying terms.

Table A5

First order term parameters

$A_{\phi}/\sum A_i =$			0.105
$-\lambda_{\phi} =$	$D_{\parallel} + D_{\perp} + D_1/b^2$	=	3.076×10^8 s^{-1}
$A_1/\sum A_i =$			0.719
$-\lambda_1 =$	$2D_{\perp} + D_1\pi^2/L^2$	=	2.928×10^6 s^{-1}
$A_3/\sum A_i =$			0.103
$-\lambda_3 =$	$2D_{\perp} + 9D_1\pi^2/L^2$	=	2.431×10^7 s^{-1}
$A_5/\sum A_i =$			0.038
$-\lambda_5 =$	$2D_{\perp} + 25D_1\pi^2/L^2$	=	6.707×10^7 s^{-1}
$A_7/\sum A_i =$			0.021
$-\lambda_7 =$	$2D_{\perp} + 49D_1\pi^2/L^2$	=	1.312×10^8 s^{-1}
$A_9/\sum A_i =$			0.014
$-\lambda_9 =$	$2D_{\perp} + 81D_1\pi^2/L^2$	=	2.167×10^8 s^{-1}

A6. The role of R_{mn} in the first order terms

Terms with all $m_i = 0$ have either $m = 0$ or $m_i' = m$. In either case it is easy to show that the m dependence of the terms inside the brackets in eq. 13 vanishes. If $n_i = 0$, the requirement $n_i' = n_i - n$ causes the n dependence to disappear. If the surviving terms with $n_i = 1$ ($L = 1$, $m = 1$) and $n_i = -1$ ($L = 1$, $m = 1$) are added as shown in eq. A6, one finds they sum to zero. Thus R_{mn} does not influence the ${}^1a_{11} + {}^1a_{1-1}$ combination needed to evaluate ${}^2a_{20}$.

The ${}^1a_{10}^{k000\cdots}$ terms (k odd) have all $n_i = 0$ and so no factors involving n occur inside the brackets in eq. 13. However, there is coupling to more structured ${}^1a_{10}$ terms of the type ${}^1a_{10}^{\{k+m \text{ or } k-m\}\cdots}$ $\{k-m \text{ or } m-k \text{ or } k+m\}$. Thus the solution for the dielectric response, or for the $L = 1$, $m = 0$ terms needed for the dynamic Kerr effect involves truncation of a hierarchy of coupled differential equations. Additional terms should be included until the solution for ${}^2a_{20}^{0000\cdots}(t)$ is unaffected to the desired accuracy of the calculation. These terms modify slightly the short time response and they decay at relatively large rates. A first approxima-

tion is to ignored them in the expression for the dynamic Kerr effect.

A7. Comments on Monte Carlo integration

With the large number of coordinates, to avoid attrition, the Metropolis algorithm is mandatory [15]. As with our calculations on disk membrane vesicles [2] configuration space was divided into a (large) finite number of cells and the calculated quantities extrapolated to zero cell size. The difference in this work is that as the algorithm is implemented, instead of estimating values for functions of one and two coordinates, we accumulate the (integral) occupancy of cells corresponding to singlet and pair distribution functions in configuration space variables. The integrals of interest (the entries of table A3 for example) are computed from the distribution functions after the algorithm has been terminated. This use of integer arithmetic is crucial to obtaining convergence in the large dimensional integrals evaluated. Furthermore any one or two particle property can be evaluated. The very large arrays (4×10^6 elements) generated are stored on the scratch disk of a VAX 8650 computer. Typical large runs required 50 h CPU.

References

1 J.A. Altig, G.E. Wesenberg and W.E. Vaughan, Biophys. Chem. 24 (1986) 221.
2 W.E. Vaughan, J. Mol. Liquids 36 (1987) 1.
3 A. Szabo, M. Haleem and D. Eden, J. Chem. Phys. 85 (1986) 7472.
4 F. Eirich, ed., Rheology, vol. 1 (Academic Press, New York, 1956).
5 M.M. Tirado, C.L. Martínez and J.G. de la Torre, J. Chem. Phys. 81 (1984) 2047.
6 P.I. Meyer and W.E. Vaughan, Biophys. Chem. 12 (1980) 329.
7 G.E. Wesenberg and W.E. Vaughan, J. Chem. Phys. 87 (1987) 4240.
8 P.G. Hoel, Introduction to mathematical statistics, 2nd edn. (John Wiley and Sons, Inc., New York, 1954).
9 G.E. Wesenberg and W.E. Vaughan, Biophys. Chem. 18 (1983) 381.
10 D.C. Rau and E. Charney, Biophys. Chem. 14 (1981) 1.
11 D.C. Rau and E. Charney, Biophys. Chem. 17 (1983) 35.
12 E. Charney, Q. Rev. Biophys. 21 (1988) 1.
13 J.D. Jackson, Classical electrodynamics (John Wiley and Sons, Inc., New York, 1962).
14 M. Abramowitz and I.A. Stegun, Handbook of mathematical functions (Dover, New York, 1972).
15 N. Metropolis, A.W. Rosenbluth, M.N. Rosenbluth, A.H. Teller and E. Teller, J. Chem. Phys. 21 (1953) 1087.